Human Molecular Genetics, 2005, Vol. 14, No. 3 **347–356**
doi:10.1093/hmg/ddi031
Advance Access published on December 8, 2004

Interactions in the network of Usher syndrome type 1 proteins

Avital Adato[1], Vincent Michel[1], Yoshiaki Kikkawa[2], Jan Reiners[3], Kumar N. Alagramam[4], Dominique Weil[1], Hiromichi Yonekawa[3], Uwe Wolfrum[2], Aziz El-Amraoui[1] and Christine Petit[1,*]

[1]Unité de Génétique des Déficits Sensoriels, INSERM U587, Institut Pasteur, 25 rue du Dr Roux, 75724 Paris cedex 15, France, [2]Department of Laboratory Animal Science, The Tokyo Metropolitan Institute of Medical Science (Rinshoken), Tokyo, Japan, [3]Institute of Zoology, University of Mainz, Germany and [4]Department of Otolaryngology-HNS, University Hospitals of Cleveland, Case Western Reserve University, Cleveland, OH, USA

Received September 28, 2004; Revised November 7, 2004; Accepted November 25, 2004

Defects in myosin VIIa, harmonin (a PDZ domain protein), cadherin 23, protocadherin 15 and sans (a putative scaffolding protein), underlie five forms of Usher syndrome type I (USH1). Mouse mutants for all these proteins exhibit disorganization of their hair bundle, which is the mechanotransduction receptive structure of the inner ear sensory cells, the cochlear and vestibular hair cells. We have previously demonstrated that harmonin interacts with cadherin 23 and myosin VIIa. Here we address the extent of interactions between the five known USH1 proteins. We establish the previously suggested sans–harmonin interaction and find that sans also binds to myosin VIIa. We show that sans can form homomeric structures and that harmonin b can interact with all harmonin isoforms. We reveal that harmonin also binds to protocadherin 15. Molecular characterization of these interactions indicates that through its binding to four of the five USH1 proteins, the first PDZ domain (PDZ1) of harmonin plays a central role in this network. We localize sans in the apical region of cochlear and vestibular hair cell bodies underneath the cuticular plate. In contrast to the other four known USH1 proteins, no sans labeling was detected within the stereocilia. We propose that via its binding to myosin VIIa and/or harmonin, sans controls the hair bundle cohesion and proper development by regulating the traffic of USH1 proteins *en route* to the stereocilia.

INTRODUCTION

Usher syndrome (USH) is the most frequent cause of hereditary deaf-blindness in humans. Three USH subtypes are clinically distinguished based on differences in the severity of hearing loss and vestibular dysfunction. Progressive visual loss due to retinitis pigmentosa with variable age of onset occurs in all the three types. All subtypes are genetically heterogeneous. USH type I (USH1), characterized by severe to profound congenital sensorineural deafness, constant vestibular dysfunction and retinitis pigmentosa with pre-pubertal onset (1), is the most severe. Seven loci (USH1A–G) have been shown to be associated with USH1 and five of the corresponding genes have been identified so far. *USH1B* encodes the actin-based motor protein myosin VIIa (2). *USH1C* encodes a PDZ domain containing protein, harmonin (3,4). Mutations in genes encoding two cadherin-related proteins, cadherin 23 and protocadherin 15, underlie *USH1D* and *USH1F*, respectively (5–8). Finally, *USH1G* encodes the putative scaffolding protein sans (9) (Fig. 1A–D).

Mouse mutants for all the known *USH1* genes have been reported; shaker1 (*sh1*) for myosin VIIa (10), deaf circler (*dfcr*) for harmonin (11), waltzer (*v*) for cadherin 23 (12,13), Ames waltzer (*av*) for protocadherin 15 (14) and Jackson shaker (*js*) for sans (15). All these mutants are deaf, exhibit vestibular dysfunction and display similar morphological abnormalities in the development of the hair bundles, the mechanotransduction receptive structure crowning the inner ear sensory cells (hair cells). The hair bundle is composed of 20–300 actin-filled rigid microvilli, named stereocilia, that contain the mechanoelectrical transduction machinery. Stereocilia are packed into rows of increasing height to form an organized and uniformly oriented hair bundle. A few of the stereocilia actin filaments extend rootlets into the cuticular

*To whom correspondence should be addressed. Tel: +33 1456888 90/93; Fax: +33 145676978; Email: cpetit@pasteur.fr

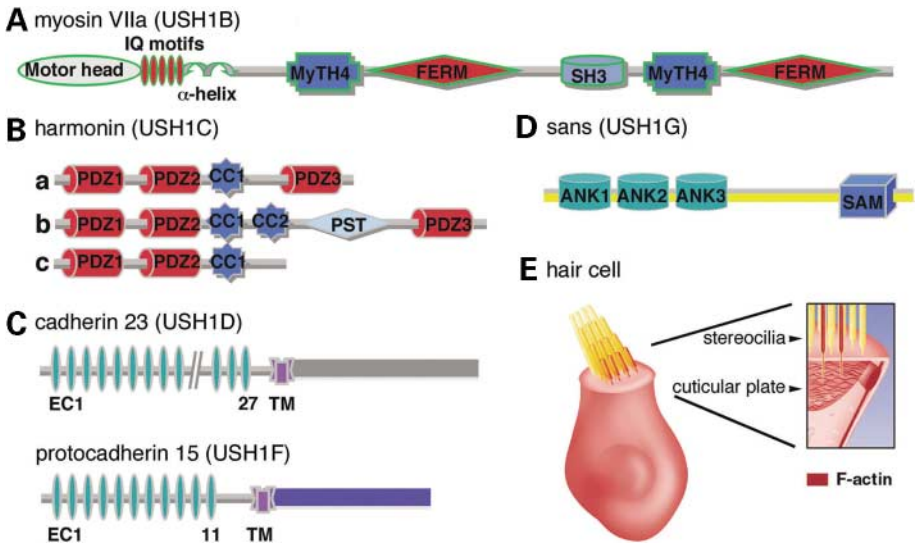

Figure 1. Schematic representation of the five known USH1 proteins and of an inner ear hair cell: (**A**) Myosin VIIa (USH1B); (**B**) harmonin (USH1C) isoforms. At least 11 isoforms are divided into three classes. Harmonin a and b isoforms contain three PDZ (postsynaptic density 95, discs large, zonula occludens-1) domains. The longest class b isoforms, contain also a second coiled coil domain (CC2), and a proline, serine, threonine (PST)-rich region. Class c, the shortest isoforms, contains only the first two PDZ domains and the first coiled coil domain. (**C**) Cadherin 23 (USH1D) and protocadherin 15 (USH1F), two cadherin-related proteins. Cadherins are integral membrane glycoproteins that mediate calcium-dependent cell–cell adhesion. Protocadherins are non-classic cadherins, which are thought to be involved in a variety of functions including neural development and formation of the synapse. (**D**) Sans (USH1G), a putative scaffolding protein that contains three ANK repeats and a SAM (sterile alpha motif) domain. (**E**) An inner ear hair cell. At the apical surface of the cell, a number of microvilli-like structures, called stereocilia, form the hair bundle. Each stereocilium contains a core of actin filaments (shown in red in the right panel). The central actin filaments of all the stereocilia are inserted into the cuticular plate, i.e. a dense meshwork of actin filaments lying beneath the apical cell surface. Indicated acronyms: FERM (4.1, ezrin, radixin, moesin); MyTH4 (myosin tail homology 4); SH3 (src homology-3), IQ (isoleucine–glutamine motifs), EC (extracellular cadherin repeats).

plate, a dense meshwork of horizontal actin filaments located beneath the apical cell surface, to which they are connected (Fig. 1E). Upon hair bundle deflection in response to sound or acceleration stimuli, all stereocilia pivot around their basal insertion points, causing opening or closing of the transduction channels, and thus fluctuations in the hair cell's membrane potential (16).

On the basis of several observations including the presence of harmonin b, cadherin 23 and myosin VIIa within the growing stereocilia, the direct interaction of harmonin with cadherin 23 and myosin VIIa and the absence of harmonin b, an F-actin binding isoform, from stereocilia in *sh1* mouse mutants, we had previously proposed that myosin VIIa is necessary for harmonin b targeting towards its stereocilia location, where harmonin b anchors cadherin 23 to the stereocilia actin core (17). This proposal is supported by the phenotypes of the two recently characterized *dfcr* mouse mutants. Although one mutant *dfcr* is defective in all harmonin isoforms (a, b and c) and the other mutant *dfcr* 2 Jackson (*dfcr 2J*) is defective only in harmonin b isoforms, both the mouse mutants exhibit the same hair bundle disorganization, also similar to the hair bundle phenotype observed in *sh1* and *v* mutants (11).

In this study, we further investigate the possible interactions between USH1 proteins. The emerging picture reveals that every USH1 protein can bind to at least one other USH1 protein. By *in vitro* binding dissection, we identified a harmonin domain that plays a key role in the network of USH1 proteins. Finally, based on sans sub-cellular localization and on its molecular interactions, as well as on the js phenotype, we propose that sans controls the targeting of USH1 proteins to the hair bundle.

RESULTS

Harmonin is a key organizer of the USH1 network

Harmonin interacts directly with cadherin 23 and myosin VIIa (17,18) (Fig. 2A). Protocadherin 15, which like harmonin, myosin VIIa and cadherin 23, has been shown to be present in the growing hair bundle (19), harbors a C-terminal class I PDZ-binding motif, TSL. We carried out binding assays to test a possible interaction between harmonin and protocadherin 15. *In vitro* translated protocadherin 15 cyto-domain bound to immobilized GST–harmonin a, whereas no binding was detected with the GST control (Fig. 2A). Significant *in vitro* binding was still observed when GST–harmonin a is incubated with a protocadherin 15 cytoplasmic fragment lacking the 64 C-terminal amino acids (data not shown). This interaction was further supported by the results of a yeast two-hybrid screening, in which the 540 C-terminal amino acids of the protocadherin 15 cytoplasmic domain were used as a bait to screen a P2–P6 inner ear sensory epithelium two-hybrid cDNA library. Five independent harmonin clones were isolated. The common region of these five clones encodes harmonin's PDZ1 and PDZ2 domains as well as harmonin's first coiled coil region, which are present in all harmonin isoforms (data not shown). Further directed yeast

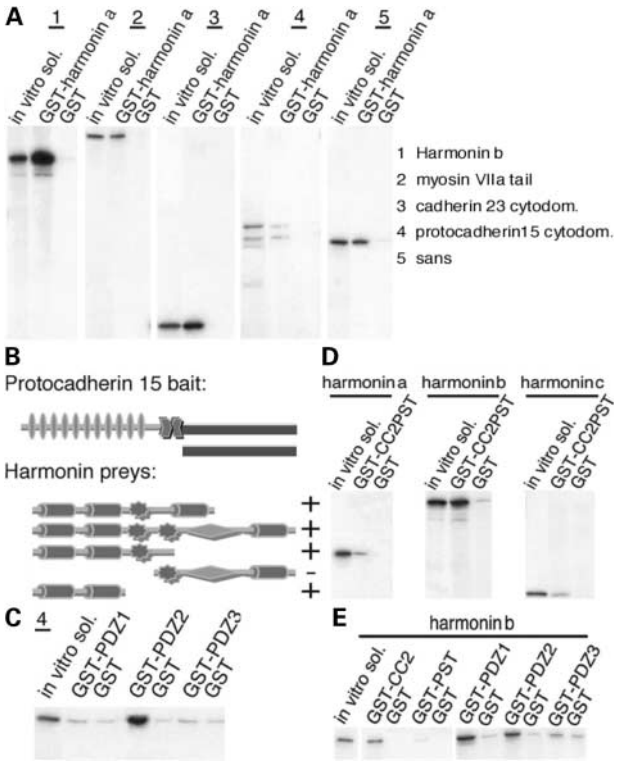

Figure 2. (**A**) Harmonin interactions. Immobilized GST–harmonin a was incubated with *in vitro* translated ^{35}S-labeled harmonin b, myosin VIIa tail, the cyto-domains of cadherin 23 and protocadherin 15 and sans. Harmonin a binds to all USH1 proteins including harmonin b. No binding is detected with the GST controls. (**B**) Schematic representation of the protocadherin 15 bait and harmonin preys used in the yeast two-hybrid assays. + indicates growth; − indicates no growth under selective pressure. (**C**) *In vitro* translated cyto-domain of protocadherin 15 was incubated with immobilized GST-tagged harmonin PDZ fragments. Only PDZ2 binds to protocadherin 15 cyto-domain. No binding is detected with PDZ1 or PDZ3. (**D**) ^{35}S-harmonin a, b and c were incubated with GST-tagged harmonin b fragment including its CC2 and PST domains and with GST control. GST–CC2PST binds to all three harmonin isoforms. (**E**) ^{35}S-harmonin b was incubated with five different GST-tagged harmonin b fragments. It binds to the CC2, PDZ1 and PDZ2 fragments. No significant binding was detected to PDZ3 or to the PST domains.

two-hybrid analysis revealed that this protocadherin 15–harmonin interaction was disrupted when harmonin's N-terminal including the PDZ1, PDZ2 and CC1 domains was deleted (Fig. 2B). Further dissection by *in vitro* assays indicates that the cytoplasmic tail of protocadherin 15 binds to harmonin's PDZ2 domain whereas no binding was observed with harmonin's PDZ1 or PDZ3 domains (Fig. 2C).

In a previous study, a yeast two-hybrid analysis indicated that the C-terminal class I PDZ—binding motif of harmonin a1 isoform binds to harmonin PDZ1 domain (18). Analysis of the harmonin–harmonin interaction by *in vitro* binding assays carried out in our study showed that a GST–harmonin b fragment including the CC2 and PST domains, present only in harmonin b, binds to the three *in vitro* translated harmonin isoforms a, b and c (Fig. 2D). Further dissection of this interaction indicated that harmonin b CC2 domain binds to representatives of all three harmonin isoform groups through their PDZ1 and PDZ2 domains (Fig. 2E). Harmonin b CC2–PST fragment did not show any binding to another three PDZ domain protein, whirlin (data not shown), which has the closest similarity to harmonin and is also localized at the tip of the hair bundle (20,21).

We have previously shown that harmonin co-localizes with sans in co-transfected HeLa cells and that in such cells harmonin b can recruit sans to the actin filaments (9). Here, we tested, by *in vitro* binding assays, whether harmonin directly interacts with sans. *In vitro* translated sans bound to immobilized GST–full length harmonin a (Fig. 2A). No binding was detected between the GST-tagged full length sans and an *in vitro* translated PDZ domain-containing fragment of Apxl (NP_766029), another PDZ protein also present in the hair cells (I. Zwaenepoel, unpublished data). Further dissection of the harmonin–sans interaction revealed that harmonin binds to sans through its PDZ1 and/or PDZ3 (but not PDZ2) domains (Fig. 3A), whereas sans binds to harmonin through its SAM domain (Fig. 3B–D; details given subsequently). Sans' C-terminal tripeptide, TEL, represents a class I PDZ-binding motif. However, *in vitro* translated harmonin a still showed binding to a GST–sansCterΔ8aa fragment lacking sans' eight C-terminal amino acids (Fig. 3B).

Thus, in addition to its interactions with myosin VIIa and cadherin 23, harmonin directly interacts also with sans via its PDZ1 and/or PDZ3 domains and with protocadherin 15 via its PDZ2 domain. Furthermore, *in vitro* assays indicate that the second coiled coil region of harmonin b can bind to PDZ1 and PDZ2 domains of all harmonin isoforms.

Sans forms homomeric structures and directly interacts with two other USH1 proteins, myosin VIIa and harmonin

SAM domains, known to be involved in protein–protein interactions, may undergo homo- or heteromerization with other SAM domains (22,23). We therefore examined by an *in vitro* binding assay whether sans molecules undergo homomerization. *In vitro* translated sans was incubated with immobilized GST–sans and with GST alone. Sans did bind to the GST–sans, whereas no binding was observed with the GST control (Fig. 3C). This interaction was further analyzed by incubation of *in vitro* translated full length sans with three immobilized GST–sans fragments: sansNter, sansCent and sansCter (Fig. 3D). Unexpectedly, no binding was observed to sansCter. The full length sans bound only to sansCent (Fig. 3E).

We then tested whether sans interacts with other USH1 proteins. In order to address the putative interaction between myosin VIIa and sans, we examined the distribution of sans and myosin VIIa in co-transfected HeLa cells. In cells producing sans and either the full length myosin VIIa or the myosin VIIa tail (amino acid 847–2215), the two proteins entirely co-localized throughout the cytoplasm (Fig. 4A–C and data not shown). To further analyze this interaction, we carried out *in vitro* binding assays. Incubation of the *in vitro* translated myosin VIIa tail with immobilized GST–sans or GST–sans fragments yielded strong binding of myosin VIIa tail to the full length sans and to sansCent (Fig. 4D). Some residual binding was also observed with the two end sans fragments sansNter and sansCter (data not shown). Further dissection

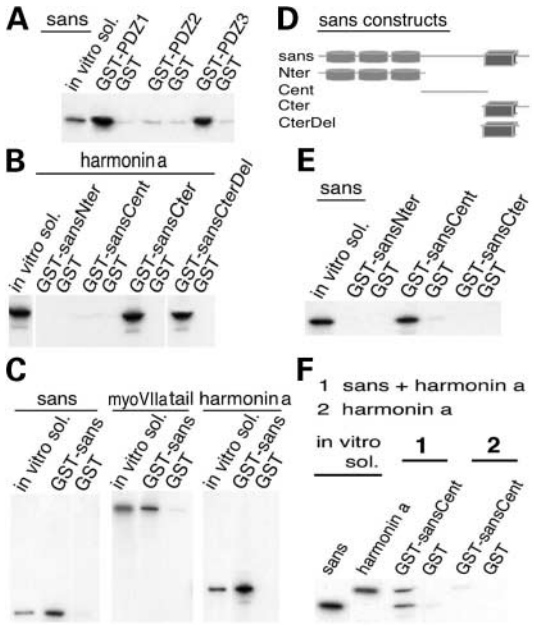

Figure 3. (**A**) *In vitro* translated full sans was incubated with immobilized GST-tagged harmonin PDZ fragments. Both PDZ1 and PDZ3 bind to the full sans. No binding is detected with PDZ2. (**B**) ^{35}S-harmonin a was incubated with the four immobilized GST-tagged sans fragments. Both sansCter (amino acid 385–461) and sansCterΔ8 (amino acid 385–453) bind to harmonin a. (**C**) GST–sans was incubated with *in vitro* translated sans, myosin VIIa tail and harmonin a. Sans binds to the three proteins, whereas no binding is detected to the GST control. (**D**) Schematic representation of sans and its four partial GST fragments. (**E**) Characterization of the sans homomerization site. Full ^{35}S-sans was incubated with three different GST-tagged sans fragments. Only the GST–sansCent (amino acid 128–385) binds to the full sans. (**F**) Pre-incubated mixture of ^{35}S-harmonin a and ^{35}S-sans, or ^{35}S-harmonin a alone were incubated with immobilized GST–sansCent fragments and with GST control. SansCent domain binds to the sans–harmonin a complexes but not to harmonin a alone.

of this interaction showed that the full length GST–sans strongly binds to the first of two MyTH4–FERM repeats of the myosin VIIa tail. Although weaker than the binding with the first myosin VIIa MyTH4–FERM repeat, significant binding was also detected between sans and a myosin VIIa tail fragment including its second MyTH4–FERM repeat (Fig. 4E and F). In contrast, no binding could be detected between sans and a C-terminal myosin XV fragment containing its SH3, MyTH4 and FERM domains (data not shown).

In vitro binding assays that were carried out to test interactions between GST–sans and the *in vitro* translated cytodomains of cadherin 23 and protocadherin 15 did not reveal any significant binding (data not shown).

Therefore, these results indicate that sans molecules can form homomers through their central region, and that sans directly interacts with the MyTH4–FERM domains of myosin VIIa and with harmonin's PDZ1 and/or PDZ3 domains via its central and SAM domains, respectively. Directed yeast two-hybrid analysis in which a library of USH1 cDNAs was screened by the full length and three partial sans baits corroborated these three sans–sans, sans–myosin VIIa and sans–harmonin interactions (data not shown).

Sans contributes to the hair bundle cohesion via an activity exerted underneath the hair bundle

We studied the distribution of sans in the mouse inner ear during hair bundle differentiation. Mouse stereocilia sprout from the apical surface of vestibular and cochlear hair cells at E13 and E15, respectively (24,25). In the cochlea, hair cell differentiation proceeds from the base to the cochlear apex and, by P4–P6, the hair bundles reach their adult shape (24). Three rabbit polyclonal antibodies directed against sans' N-terminal, center and SAM domain regions (MP1, MP2 and MP3, respectively) were generated. The three antibodies recognized the over expressed myc-tagged sans in transfected HeLa cells. However, MP1, which was generated against the first 46 amino acids of the protein, gave the strongest signal among the three tested antibodies (data not shown). From P1 onwards, sans was detected in all types of inner ear hair cells as well as in some of the supporting cells. Detailed confocal microscopy analysis showed intense sans immunoreactivity at the apical part of cochlear (inner and outer) and vestibular hair cell bodies underneath the cuticular plate (Fig. 5). In cochlear outer hair cells (OHC), this apical labeling was more concentrated at the proximity of the kinocilium basal body (Fig. 5A–G), where the cuticular plate gets thinner (26). Sans labeling beneath the kinocilium basal body of OHCs becomes more robust from P3 to P15. Such labeling concentration was not observed in cochlear inner hair cells (IHC) (Fig. 5A and D). Weak diffusely distributed sans immunoreactivity was also detected in the cytoplasm of hair cells bodies with stronger labeling at the synaptic region (Fig. 5E–G). No co-localization was found between sans and F-actin staining and sans immunoreactivity could not be detected in the stereocilia (Fig. 5A, C–E and G). However, the kinocilium of P3 OHCs was labeled (Fig. 5A–C). At all the tested stages, sans immunoreactivity was stronger in the OHCs than in the IHCs (Fig. 5A and D). This difference between OHCs and IHCs correlates with the previously described js phenotype, in which at all the tested stages abnormal stereocilia configuration was observed in cochlear OHCs whereas cochlear IHCs seemed to be preserved (27).

As shown here and in previous studies, sans, harmonin and myosin VIIa are all present within the apical region of mice cochlear hair cells during hair bundle development (17,28) (Fig. 5H and J). As sans was shown to form homomers via its central region and to bind to harmonin via its SAM domain, we explored whether a triple sans–sans–harmonin complex could be detected *in vitro*. In this assay, GST–sansCent was incubated with either a pre-incubated mixture of *in vitro* translated full sans and harmonin a or harmonin a alone. GST–sansCent bound to the sans–harmonin complexes. In contrast, no binding was detected with harmonin a alone (Fig. 3F). We also carried out similar assays in order to test putative *in vitro* formation of sans–harmonin–myosin VIIa complexes. GST–sansCent and GST–sansCter were incubated each with either a pre-incubated mixture of myosin VIIa and harmonin a or myosin VIIa alone or harmonin a alone. Binding was detected only with myosin VIIa or harmonin a alone, whereas neither of the tested GST–sans fragments bound to harmonin–myosin VIIa complexes (data not shown). Together, these triple binding assays suggest

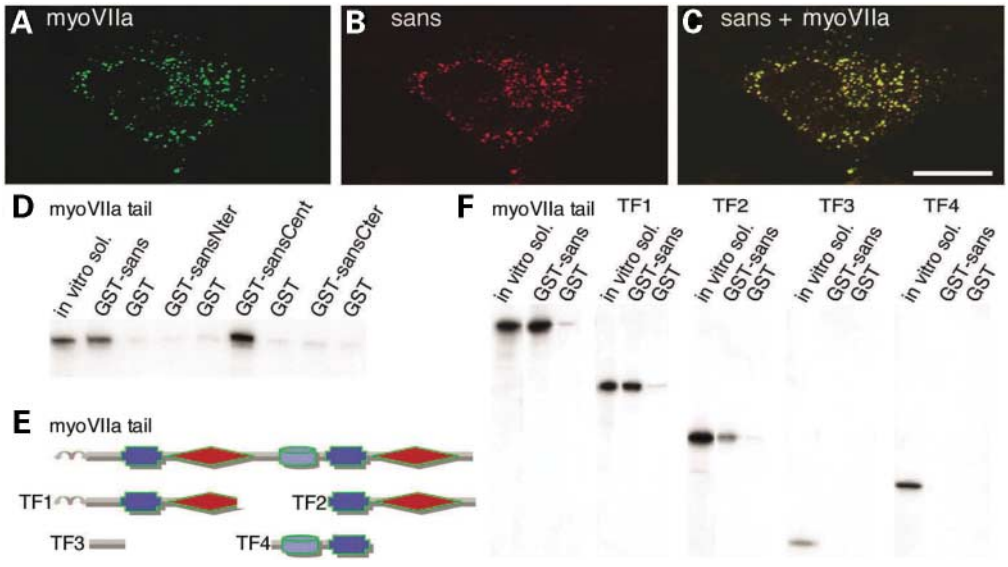

Figure 4. (**A**–**C**) Sans associates with myosin VIIa in co-transfected cells. In HeLa cells producing myosin VIIa (A) and sans (B), the two proteins show identical distributions throughout the cell (C). (**D**–**F**) Characterization of the sans–myosin VIIa binding sites. (D) *In vitro* translated ^{35}S-myosin VIIa tail was incubated with GST-tagged full sans and three sans fragments. The full length sans and sansCent fragment show significant binding with the myosin VIIa tail. (E) Schematic representation of the *in vitro* translated myosin VIIa tail and the four tail fragments (TF1–TF4). (F) *In vitro* translated entire myosin VIIa tail and tail fragments were incubated with GST–sans and GST control. The full myosin VIIa tail, and two of the tail fragments including the myosin VIIa MyTH4–FERM repeats (TF1 and TF2) bind to the GST–sans. Sans bindings with the entire tail and with TF1, including myosin VIIa first MyTH4–FERM repeat, are stronger than its binding with TF2, including the second MyTH4–FERM repeat. No binding is detected with TF3 or TF4 including the region between the α-helix and the first MyTH4 domain, and the SH3 and second MyTH4 domains, respectively.

that sans homomers can form complexes with harmonin, whereas myosin VIIa–harmonin complexes cannot interact with sans.

DISCUSSION

We have previously shown that harmonin b interacts with cadherin 23 and myosin VIIa, which are all present in the developing hair bundle (17). In this study, we deciphered additional layers of the USH1 protein network (Fig. 6A–D) by demonstrating the existence of three new USH1 interactions: sans–sans, sans–myosin VIIa and harmonin–protocadherin 15, and by establishing and dissecting the previously suggested sans–harmonin interaction (9). As a result of this, we reveal the key role of harmonin's PDZ1 domain in the formation of most harmonin interactions. Mutations in genes encoding the USH1 proteins give rise to a common phenotype of deafness and disorganized hair bundles in all the corresponding mouse mutants (10–12,14,15). Different from all the other USH1 proteins which are present in the growing stereocilia (11,17,19), sans is absent from the hair bundle. However, like myosin VIIa, harmonin and protocadherin 15, sans is concentrated beneath the stereocilia, in the apical part of inner ear hair cells' bodies.

Sans is a putative scaffolding protein containing three ankyrin (ANK) repeats, a SAM domain and a C-terminal class I PDZ-binding consensus motif (9,15). ANK repeats were originally found to link specific proteins to the membrane-associated spectrin–actin cytoskeleton in the human erythrocyte, and subsequently described in a variety of vertebrate proteins. ANK repeat proteins carry out a wide variety of biological activities such as membrane skeleton organization, ionic transport, maintenance of cell polarity as well as cell–cell adhesion regulation (29,30). None of the sans interactions identified in this work involves its ANK repeats. SAM domains are putative protein-interaction modules composed of 60–70 amino acids, which were originally identified in yeast and subsequently found in a variety of proteins (31). These domains have been shown to form homo- and hetero-oligomers and to mediate specific protein–protein interactions (32). However, the sans SAM domain was not found to be responsible for sans homomerization, but was shown to bind to harmonin PDZ1 and/or PDZ3 domains (Fig. 3A and B). Sans homomerization involves its central region (Fig. 3E), which also takes part in the sans–myosin VIIa interaction (Fig. 4D). This indicates the existence of two distinct and independent interaction sites along the sans molecule, its center and its SAM domains, which is consistent with the *in vitro* formation of a sans–sans–harmonin triple complex (Fig. 3F).

The C-terminal sequence of sans harbors a class I PDZ-binding motif, TEL. Although at first, PDZ's binding specificity appeared to involve only binding to the C-terminal of interacting partners, it is now recognized that PDZ domains interact with greater versatility, namely, through PDZ–PDZ interactions, as well as through binding to other internal peptide sequences and even to lipids such as phosphatidylinositol 4,5-bisphosphate (PIP2) (33,34). Remarkably, with the exception of myosin VIIa, four of the USH1 proteins harbor class I PDZ-binding motifs at their C-terminal ends. However, harmonin's *in vitro* interactions with either of

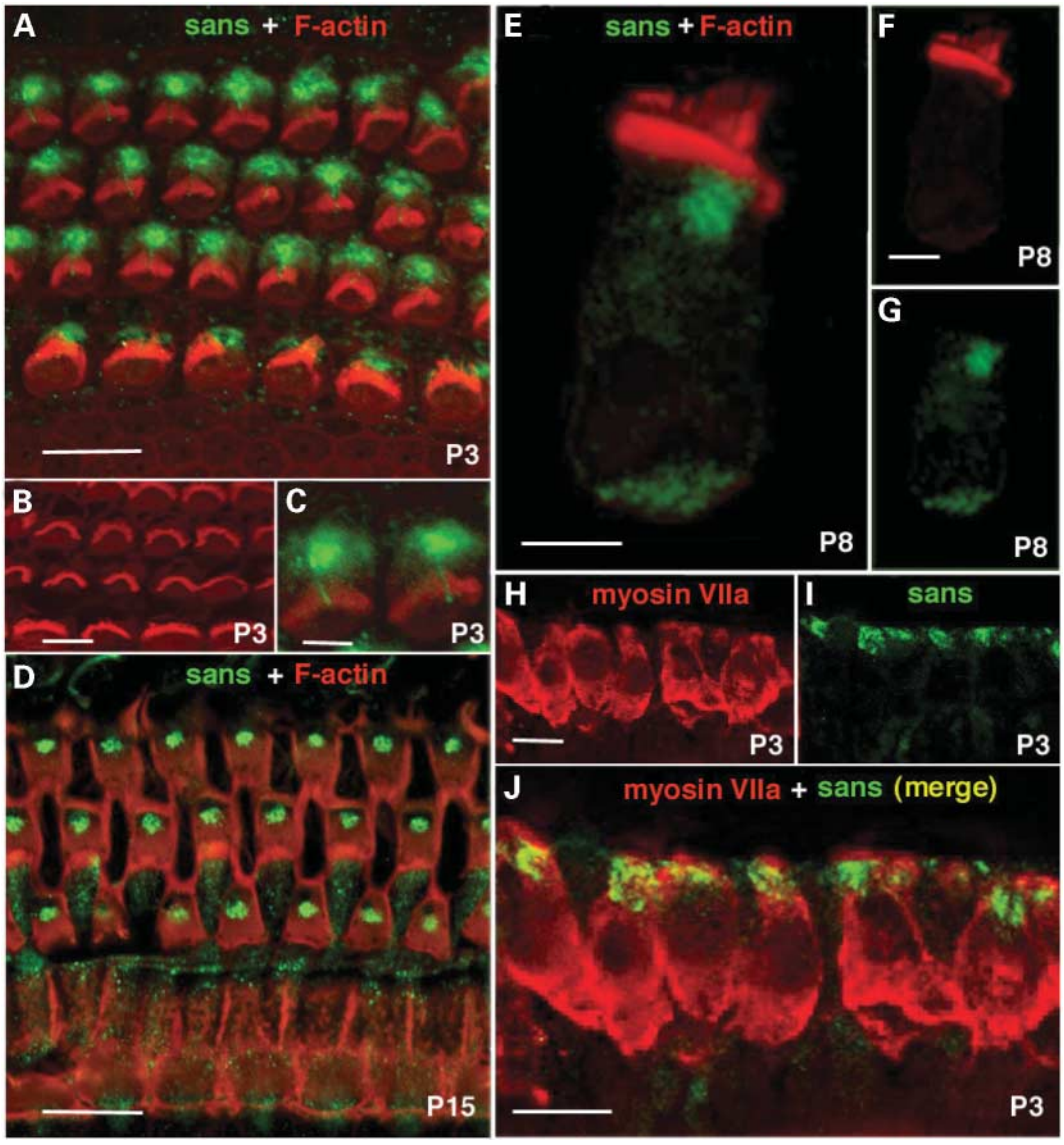

Figure 5. Immunolocalization and confocal microscopy of sans in the mouse organ of corti and vestibular sensory epithelia. (**A**) Using the rabbit anti-sans MP1, sans was detected in P3 mouse cochlea at the apical part OHCs and IHCs. Double staining of sans and F-actin revealed no co-localization of these proteins. (**B**) Rhodamine–phalloidin staining in P3 cochlear hair cells. (**C**) A small extension of sans labeling into the center the hair bundle of P3 OHCs where no labeling of actin is observed, indicate the probable localization of sans also in the kinocilium of these cochlear OHCs. (**D**) Double staining of sans and F-actin in P15 mouse cochlea revealed no co-localization of these proteins. No sans staining is visible beneath the kinocilium basal body of IHCs whereas in OHCs most sans staining is concentrated at this region. Sans immunoreactivity delineates pillar cells also. (**E**) Double staining of sans and F-actin in a P8 single cochlear hair cell. (**F**) Rhodamine–phalloidin staining of a P8 single cochlear hair cell. (**G**) Sans immunoreactivity as labeled in a P8 single cochlear hair cell. (**H**) Myosin VIIa staining in P3 mouse vestibule delineates the whole hair cells. (**I**) Sans staining in P3 mouse vestibule is intense at the apical part of the hair cells. (**J**) Sans is partially co-localized with myosin VIIa at the apical part of mouse P3 vestibular hair cells.

these proteins was not disrupted by the deletion of their C-terminal PDZ-binding motifs (18, this manuscript). This therefore reveals that harmonin's PDZ interactions with the USH1 proteins involves more than just the classical binding of C-terminal motifs. The cytoplasmic region of cadherin 23 contains a stretch of amino acids (3184–3307) with significant homology to a domain in the adaptor protein Ril that functions as an internal PDZ-binding motif (18). The harmonin b CC2 region, which was shown to interact with harmonin's PDZ1 and PDZ2 domains, contains an SEV amino acid motif at positions 708–710. Such an S/T-X-V internal PDZ-interacting motif was reported in the *Drosophila* transient receptor potential Ca^{2+} channel that has been shown to bind to the PDZ domain of the *Drosophila* InaD photoreceptor protein (35). Two similar S/T-X-V motifs could be detected along the cyto-domain of protocadherin 15, namely SFV (amino acid 1521–1523) and TQV (amino acid 1563–1566). These two motifs, if harbored in a proper structural context, might be involved in the harmonin–PDZ-binding. No putative internal PDZ-binding motif could be detected in

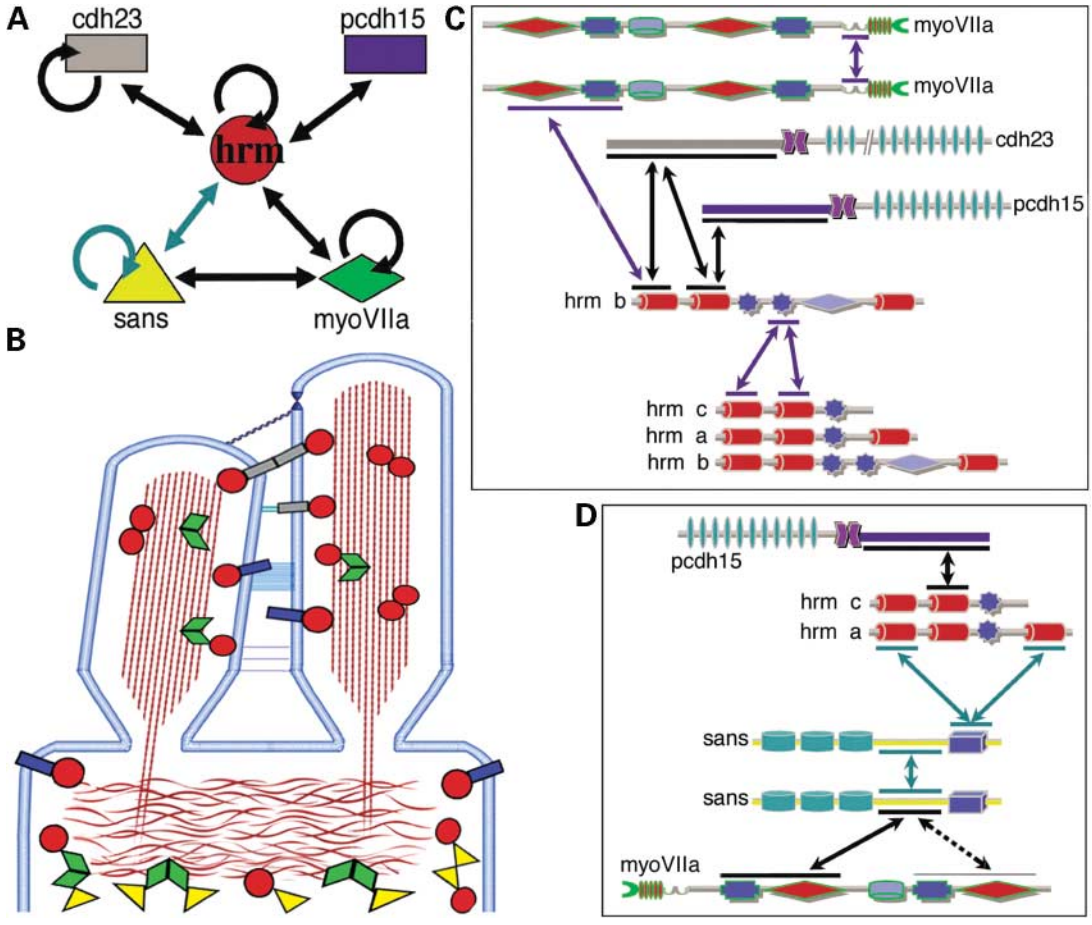

Figure 6. (**A**) Summary of the interactions within the USH1 proteins network. (**B**) Schematic diagram illustrating the type of known interactions in the USH1 protein network and the positions in the hair cell where these interactions can take place, in the hair bundle or beneath the cuticular plate. (**C**) Binding sites of interactions taking place in the stereocilia. (**D**) Binding sites of interactions taking place beneath the cuticular plate. Green arrows indicate interactions within the tripartite sans–sans–harmonin complex. Purple arrows indicate potentially non-excluding interactions. Abbreviations: cdh23, cadherin 23; pcdh15, protocadherin 15; hrm, harmonin; myoVIIa, myosin VIIa.

the sans SAM domain, thus indicating the presence of a yet uncharacterized PDZ-binding motif along this sequence. The existence of at least one additional putative internal PDZ-binding site along the sequence of these four USH1 proteins suggests that one of these sites may be implicated in an interaction with another PDZ protein. Alternatively, the specific *in vivo* recruitment of these PDZ domain binding proteins may require the participation of more than one protein–protein interaction site. The involvement of harmonin PDZ1 in most USH1 protein interactions (i.e. harmonin–harmonin, harmonin–myosin VIIa, harmonin–sans as well as harmonin–cadherin 23) indicates that these proteins are not likely to concomitantly interact with harmonin. The competitive nature of harmonin interactions with at least some of the USH1 proteins is further supported by the triple *in vitro* binding assays in which harmonin–myosin VIIa complexes did not bind to tested sans fragments including the sans–harmonin or sans–myosin VIIa binding sites. Therefore, the expression of harmonin isoforms (17,36) and other USH1 proteins in defined subcellular localization at a given developmental stage, as well as the relative affinities of each interaction, will eventually dictate the composition and dynamics of harmonin complexes that will form at a given time and cellular emplacement. Figure 6 summarizes and schematizes the various USH1 proteins interactions. We have previously suggested that cadherin 23, which we found to be present in the stereocilia only during its growth, could form embryonic interstereociliar links that are anchored to the actin core by harmonin b (17). Since then cadherin 23 has been suggested to be an essential tip link component required for hair-cell mechanotransduction (37,38). This apparent contradiction concerning the persistence of cadherin 23 in adult stereocilia could be settled if the antibodies used in the two studies are labeling different cadherin 23 isoforms. Protocadherin 15 is detected all along the stereocilia as soon as these become distinguishable at the apical surface of hair cells (19). Therefore, along the same lines as with cadherin 23, the protocadherin 15–harmonin binding indicates a similar mechanism of protocadherin 15 anchoring to the actin core during hair bundle development (17,19). Whether protocadherin 15 or any of the other USH1 proteins have a crucial role also in the cohesion of adult hair bundle is yet unknown.

A dense population of vesicles has been detected by EM around the cuticular plate, situated in a narrow area of the hair cell's cytoplasm separating the cuticular plate actin matrix and the actin ring associated with the apical junctional complex. In vestibular hair cells, these vesicles were shown to extend into an actin-free region at the base of the kinocilium, where microtubules are also found (26). These vesicles are likely to be part of a traffic system responsible for exo- and endo-cytosis exchanges between the hair cell's cytoplasm and the apical plasma membrane. So far, sans is the only USH1 protein that could not be detected in the stereocilia. However, it displays intense labeling under the cuticular plate that anchors the stereocilia actin filaments, and in cochlear OHCs sans immunoreactivity is especially robust around the base of the kinocilium basal body. This expression pattern overlaps with the localization of the previously described trafficking vesicles (26); myosin VIIa and harmonin staining are also particularly strong at that same cellular emplacement (17,19,28) (Fig 5H–J). Therefore, on the basis of sans interactions and on its localization, we propose that via its binding to myosin VIIa and/or harmonin, sans may directly or indirectly regulate the trafficking of USH1 proteins in their route to the stereocilia. Within this yet unknown route of components from the endoplasmic reticulum to the hair bundle, sans and myosin VIIA could be involved in vesicular trafficking along the microtubules and actin filaments, respectively, and through their interactions they might take part in the translocation of vesicles between microtubules and actin filaments tracks.

Various findings indicate that in addition to their role in the proper development of the hair bundle, USH1 proteins might be involved also in other hair cells functions. One of the original shaker1 mouse mutants, homozygous for the *Myo7a*^{sh1} allele, exhibits abnormal cochlear responses although the development of its hair bundle's stereocilia seems normal (39). Myosin VIIa has also been localized in pre-synaptic junctions of inner ear hair cells (40), whereas in the retina, three of the USH1 proteins (harmonin, myosin VIIa and cadherin 23) were shown to be co-localized in photoreceptors synapses (36). Finally, in this study also sans was localized to the synaptic region of the hair cells (Fig. 5E–G). Thus, we suggest that the proteins comprising the USH1 network may also take part in the organization and/or function of hair cells/photoreceptors synapses.

MATERIALS AND METHODS

Yeast two-hybrid screenings

Yeast two-hybrid screening was performed on the inner ear two-hybrid cDNA library (17) using the cytoplasmic region of protocadherin 15 (amino acid 1403–1943) as bait. Directed two-hybrid assays were carried out to analyze sans and protocadherin 15 interactions. Full and fragmented sans constructs as well as the C-terminal cytoplasmic region of protocadherin 15 (amino acid 1391–1943) were cloned into the Gal4 DNA-binding domain contained in the pGBKT7 vector (Clontech) as baits. Myosin VIIa, harmonin, cadherin 23, protocadherin 15 and sans constructs were expressed from pGBKT7 (Clontech) as preys. Protein–protein interactions were determined as yeast growth under selective pressure and X-gal blue/white assay (41).

Expression constructs

The cytoplasmic region of protocadherin 15 (NM 023115; amino acid 1403–1943) was amplified from a mouse inner ear cDNA library and cloned into pCMVtag3B (Myc tag, Stratagene) and pcDNA (no tag, Invitrogen) for expression in HeLa cells, and into pGex-4T1 (GST tag, Amersham) for protein production. cDNAs encoding partial sans fragments, i.e. N-terminal ANK repeats (amino acid 1–128, sansNter), central region (amino acid 128–385, sansCent), SAM domain C-terminal (amino acid 386–461, sansCter) and a truncated sansCter in which the last eight amino acid are deleted (amino acid 386–453, sansCterΔ8), as well as fragments of protocadherin 15 including its C-terminal cyto-domain (amino acid 1403–1943) and a truncated cyto-domain (amino acid 1403–1879) were subcloned into pCMV-tag3B and pGex-4T1. Myosin tail, harmonin and cadherin 23 constructs were obtained as described (17). The full sans construct was obtained as described (9).

Binding experiments

The *in vitro* binding assays were carried out using GST-tagged fusion proteins as follows: radiolabeled proteins were translated *in vitro* with the T7-coupled transcription–translation system (Promega) according to the manufacturer's instructions. To test sans and harmonin interactions with other USH1 proteins, a bacterial lysate containing GST-constructs of either sans or harmonin, or GST alone, was incubated with pre-equilibrated glutathione–Sepharose beads (Pharmacia) for 90 min at 4°C on a rotating wheel. The beads were washed three times with binding buffer [Phosphate-buffered saline (PBS) with 5% glycerol, 5 mM $MgCl_2$ and 0.1% Triton X-100] supplemented with an EDTA free protease inhibitor cocktail (Roche), and then incubated with ^{35}S-labeled sans–harmonin–myosin VIIa tail–cadherin 23–protocadherin 15 for 3 h, at 4°C on a rotating wheel. The beads were then washed four times with binding buffer supplemented with 150 mM NaCl, and bound proteins were resuspended in 20 µl 2× SDS sample buffer, and then analyzed on a 4–12% SDS–PAGE.

Antibody production

Three rabbit polyclonal antibodies to sans were generated against different peptides derived from the murine protein: MP1 against the first 46 N-terminal amino acids, MP2 against a petide sequence in the central region of sans (amino acid 354–372) and MP3 against a peptide in the C-terminal SAM region (amino acid 421–439). Specificity of the affinity-purified antibodies was assayed by immunofluorescence and immunoblot analysis. Substitution of the pre-immune sera for the purified anti-sans antibodies and pre-adsorption of the antibodies with the corresponding antigens were used as negative controls. Antibodies to harmonin a and b as well as to myosin VIIa and cadherin 23 have been previously described (17).

Cell lines and immunofluorescence analysis

HeLa cell lines were cultured in Dulbecco's modified Eagle medium (DMEM) supplemented with 10% fetal calf serum. Cells were collected 2 days after transfection by effectene transfection reagent (Qiagen) and processed for immunocytofluorescence as described (42). Briefly, HeLa cells were incubated for 15 min with 50 mM NH_4Cl in PBS, then washed in 0.01% saponin in PBS. The cells were incubated for 1 h in 10% goat serum in PBS, and then with the anti-myc and/or anti-protein antibodies for 1 h at room temperature, followed by the secondary antibody (1 h at room temperature). The mouse monoclonal anti-myc antibody used in our experiments is clone 9E10 (Santa Cruz). Rhodamine–phalloidin (Sigma) staining was used to visualize actin filaments.

Cochlear dissections and staining

Mouse tissues and inner ears were fixed and treated for immunofluorescence as previously described (43,44). For whole mount preparations of the organ of Corti, mouse inner ears were fixed and decalcified, then half turns of the cochlea were carefully dissected to separate the organ of Corti and immediate surrounding tissues. Whole organs of Corti were then used for indirect immunofluorescence (43). In order to obtain a single hair cell staining, the isolated organ of corti was collected in 50 μl PBS and 50 μl of 10% trypsine at room temperature, and was slowly mechanically disassembled during 4 min. In total, 100 μl of fetal calf serum was added for the neutralization of the trypsin. The mixture was then sifted on Cell-Tak™ (Becton Dickinson) coated compartmentalized glass (Labtech) and fixed with 4% PFA and processed for immunocytofluorescence as described (42). Stained tissues sections, whole mount preparations and single cell mixtures were analyzed on a conventional epifluorescent microscope (Leica) or a laser scanning confocal microscope (LSM-540; Zeiss).

ACKNOWLEDGEMENTS

We thank J.P. Hardelin for critical reading of the manuscript, J. Levilliers for her inexhaustible help, B. Boëda and I. Zwaenepoel for providing harmonin and myosin VIIa constructs, respectively. We thank Darrell Pitts in K.A.'s laboratory for technical assistance. This work was supported by grants from the R. and G. Strittmatter Foundation, Retina-France, the A. and M. Suchert Forschung contra Blindheit-Initiative Usher Syndrome, Foundation pour la Recherche Médicale ARS 2000 and by an NIDCD grant RO1 DC05385 to K.A. A.A.'s postdoctoral fellowship is granted by the Pasteur–Weizmann Foundation.

REFERENCES

1. Petit, C. (2001) Usher syndrome: from genetics to pathogenesis. *Annu. Rev. Genom. Hum. Genet.*, **2**, 271–297.
2. Weil, D., Blanchard, S., Kaplan, J., Guilford, P., Gibson, F., Walsh, J., Mburu, P., Varela, A., Levilliers, J., Weston, M.D. *et al.* (1995) Defective myosin VIIA gene responsible for Usher syndrome type 1B. *Nature*, **374**, 60–61.
3. Bitner-Glindzicz, M., Lindley, K.J., Rutland, P., Blaydon, D., Smith, V.V., Milla, P.J., Hussain, K., Furth-Lavi, J., Cosgrove, K.E., Shepherd, R.M. *et al.* (2000) A recessive contiguous gene deletion causing infantile hyperinsulinism, enteropathy and deafness identifies the Usher type 1C gene. *Nat. Genet.*, **26**, 56–60.
4. Verpy, E., Leibovici, M., Zwaenepoel, I., Liu, X.-Z., Gal, A., Salem, N., Mansour, A., Blanchard, S., Kobayashi, I., Keats, B.J.B. *et al.* (2000) A defect in harmonin, a PDZ domain-containing protein expressed in the inner ear sensory hair cells, underlies Usher syndrome type 1C. *Nat. Genet.*, **26**, 51–55.
5. Bolz, H., von Brederlow, B., Ramirez, A., Bryda, E.C., Kutsche, K., Nothwang, H.G., Seeliger, M., Salcedo Cabrera, M.d.C., Vila, M.C., Molina, O.P. *et al.* (2001) Mutations of *CDH23*, encoding a new member of the cadherin gene family, causes Usher syndrome type 1D. *Nat. Genet.*, **27**, 108–112.
6. Bork, J.M., Peters, L.M., Riazuddin, S., Bernstein, S.L., Ahmed, Z.M., Ness, S.L., Polomeno, R., Ramesh, A., Schloss, M., Srisailpathy, C.R.S. *et al.* (2001) Usher syndrome 1D and nonsyndromic autosomal recessive deafness DFNB12 are caused by allelic mutations of the novel cadherin-like gene *CDH23*. *Am. J. Hum. Genet.*, **68**, 26–37.
7. Ahmed, Z.M., Riazuddin, S., Bernstein, S.L., Ahmed, Z., Khan, S., Griffith, A.J., Morell, R.J., Friedman, T.B., Riazuddin, S. and Wilcox, E.R. (2001) Mutations of the protocadherin gene *PCDH15* cause Usher syndrome type 1F. *Am. J. Hum. Genet.*, **69**, 25–34.
8. Alagramam, K.N., Yuan, H., Kuehn, M.H., Murcia, C.L., Wayne, S., Srisailpathy, C.R.S., Lowry, R.B., Knaus, R., Van Laer, L., Bernier, F.P. *et al.* (2001) Mutations in the novel protocadherin *PCDH15* cause Usher syndrome type 1F. *Hum. Mol. Genet.*, **10**, 1709–1718.
9. Weil, D., El-Amraoui, A., Masmoudi, S., Mustapha, M., Kikkawa, Y., Lainé, S., Delmaghani, S., Adato, A., Nadifi, S., Ben Zina, Z. *et al.* (2003) Usher syndrome type IG (USH1G) is caused by mutations in the gene encoding SANS, a protein that associates with the USH1C protein, harmonin. *Hum. Mol. Genet.*, **12**, 463–471.
10. Gibson, F., Walsh, J., Mburu, P., Varela, A., Brown, K.A., Antonio, M., Beisel, K.W., Steel, K.P. and Brown, S.D.M. (1995) A type VII myosin encoded by the mouse deafness gene *Shaker-1*. *Nature*, **374**, 62–64.
11. Johnson, K.R., Gagnon, L.H., Webb, L.S., Peters, L.L., Hawes, N.L., Chang, B. and Zheng, Q.Y. (2003) Mouse models of USH1C and DFNB18: phenotypic and molecular analyses of two new spontaneous mutations of the *Ush1c* gene. *Hum. Mol. Genet.*, **12**, 3075–3086.
12. Di Palma, F., Holme, R.H., Bryda, E.C., Belyantseva, I.A., Pellegrino, R., Kachar, B., Steel, K.P. and Noben-Trauth, K. (2001) Mutations in *Cdh23*, encoding a new type of cadherin, cause stereocilia disorganization in waltzer, the mouse model for Usher syndrome type 1D. *Nat. Genet.*, **27**, 103–107.
13. Wilson, S.M., Householder, D.B., Coppola, V., Tessarollo, L., Fritzsch, B., Lee, E.C., Goss, D., Carlson, G.A., Copeland, N.G. and Jenkins, N.A. (2001) Mutations in Cdh23 cause nonsyndromic hearing loss in waltzer mice. *Genomics*, **74**, 228–233.
14. Alagramam, K.N., Murcia, C.L., Kwon, H.Y., Pawlowski, K.S., Wright, C.G. and Woychik, R.P. (2001) The mouse Ames waltzer hearing-loss mutant is caused by mutation of *Pcdh15*, a novel protocadherin gene. *Nat. Genet.*, **27**, 99–102.
15. Kikkawa, Y., Shitara, H., Wakana, S., Kohara, Y., Takada, T., Okamoto, M., Taya, C., Kamiya, K., Yoshikawa, Y., Tokano, H. *et al.* (2003) Mutations in a new scaffold protein Sans cause deafness in Jackson shaker mice. *Hum. Mol. Genet.*, **12**, 453–4561.
16. Hudspeth, A.J. (1997) Mechanical amplification of stimuli by hair cells. *Curr. Opin. Neurobiol.*, **7**, 480–486.
17. Boëda, B., El-Amraoui, A., Bahloul, A., Goodyear, R., Daviet, L., Blanchard, S., Perfettini, I., Fath, K.R., Shorte, S., Reiners, J. *et al.* (2002) Myosin VIIa, harmonin, and cadherin 23, three Usher I gene products, cooperate to shape the sensory hair cell bundle. *EMBO J.*, **21**, 6689–6699.
18. Siemens, J., Kazmierczak, P., Reynolds, A., Sticker, M., Littlewood-Evans, A. and Muller, U. (2002) The Usher syndrome proteins cadherin 23 and harmonin form a complex by means of PDZ-domain interactions. *Proc. Natl Acad. Sci. USA*, **99**, 14946–14951.
19. Ahmed, Z.M., Riazuddin, S., Ahmad, J., Bernstein, S.L., Guo, Y., Sabar, M.F., Sieving, P., Riazuddin, S., Griffith, A.J., Friedman, T.B. *et al.* (2003) *PCDH15* is expressed in the neurosensory epithelium of the eye and ear and mutant alleles are responsible for both USH1F and DFNB23. *Hum. Mol. Genet.*, **12**, 3215–3223.

20. Mburu, P., Mustapha, M., Varela, A., Weil, D., El-Amraoui, A., Holme, R.H., Rump, A., Hardisty, R.E., Blanchard, S., Coimbra, R.S. *et al.* (2003) Defects in whirlin, a PDZ domain molecule involved in stereocilia elongation, cause deafness in the whirler mouse and families with mutations in DFNB31. *Nat. Genet.*, **34**, 421–428.
21. Delprat, B., Michel, V., Goodyear, R., Yamasaki, Y., Michalski, N., El-Amraoui, A., Perfettini, I., Legrain, P., Richardson, G., Hardelin, J.-P. and Petit, C. (2005) Myosin XVa and whirlin, two deafness gene products required for hair bundle growth, are located at the stereocilia tips and interact directly. *Hum. Mol. Genet.*, **14**, 401–410.
22. Schultz, J., Ponting, C.P., Hofmann, K. and Bork, P. (1997) SAM as a protein interaction domain involved in developmental regulation. *Protein Sci.*, **6**, 249–253.
23. Stapleton, D., Balan, I., Pawson, T. and Sicheri, F. (1999) The crystal structure of an Eph receptor SAM domain reveals a mechanism for modular dimerization. *Nat. Struct. Biol.*, **6**, 44–49.
24. Nishida, Y., Rivolta, M.N. and Holley, M.C. (1998) Timed markers for the differentiation of the cuticular plate and stereocilia in hair cells from the mouse inner ear. *J. Comp. Neurol.*, **395**, 18–28.
25. Denman-Johnson, K. and Forge, A. (1999) Establishment of hair bundle polarity and orientation in the developing vestibular system of the mouse. *J. Neurocytol.*, **28**, 821–835.
26. Kachar, B., Battaglia, A. and Fex, J. (1997) Compartmentalized vesicular traffic around the hair cell cuticular plate. *Hear Res.*, **107**, 102–112.
27. Kitamura, K., Kakoi, H., Yoshikawa, Y. and Ochikubo, F. (1992) Ultrastructural findings in the inner ear of Jackson shaker mice. *Acta Otolaryngol. (Stockh.)*, **112**, 622–627.
28. Hasson, T., Gillespie, P.G., Garcia, J.A., MacDonald, R.B., Zhao, Y., Yee, A.G., Mooseker, M.S. and Corey, D.P. (1997) Unconventional myosins in inner-ear sensory epithelia. *J. Cell Biol.*, **137**, 1287–1307.
29. Sedgwick, S.G. and Smerdon, S.J. (1999) The ankyrin repeat: a diversity of interactions on a common structural framework. *Trends Biochem. Sci.*, **24**, 311–316.
30. Hryniewicz-Jankowska, A., Czogalla, A., Bok, E. and Sikorsk, A.F. (2002) Ankyrins, multifunctional proteins involved in many cellular pathways. *Folia Histochem. Cytobiol.*, **40**, 239–249.
31. Ponting, C.P. (1995) SAM: a novel motif in yeast sterile and *Drosophila* polyhomeotic proteins. *Protein Sci.*, **4**, 1928–1930.
32. Kyba, M. and Brock, H.W. (1998) The SAM domain of polyhomeotic, RAE28, and scm mediates specific interactions through conserved residues. *Dev. Genet.*, **22**, 74–84.
33. Zimmermann, P., Meerschaert, K., Reekmans, G., Leenaerts, I., Small, J.V., Vandekerckhove, J., David, G. and Gettemans, J. (2002) PIP(2)-PDZ domain binding controls the association of syntenin with the plasma membrane. *Mol. Cell*, **9**, 1215–1225.
34. Nourry, C., Grant, S.G. and Borg, J.P. (2003) PDZ domain proteins: plug and play! *Sci STKE*, **2003**, RE7.
35. Shieh, B.H. and Zhu, M.Y. (1996) Regulation of the TRP Ca^{2+} channel by INAD in *Drosophila* photoreceptors. *Neuron*, **16**, 991–998.
36. Reiners, J., Reidel, B., El-Amraoui, A., Boëda, B., Huber, I., Petit, C. and Wolfrum, U. (2003) Differential distribution of harmonin isoforms and their possible role in Usher-1 protein complexes in mammalian photoreceptor cells. *Invest. Ophthalmol. Visual Sci.*, **44**, 5006–5015.
37. Siemens, J., Lillo, C., Dumont, R.A., Reynolds, A., Williams, D.S., Gillespie, P.G., Muller, U. (2004) *Cadherin 23* is a component of the tip link in hair-cell stereocilia. *Nature*, **428**, 950–955.
38. Söllner, C., Rauch, G.-J., Siemens, J., Geisler, R., Schuster, S.C., Müller, U. and Nicolson, T. (2004) Mutations in *cadherin 23* affect tip links in zebrafish sensory hair cells. *Nature*, **428**, 955–959.
39. Self, T., Mahony, M., Fleming, J., Walsh, J., Brown, S.D. and Steel, K.P. (1998) Shaker-1 mutations reveal roles for myosin VIIA in both development and function of cochlear hair cells. *Development*, **125**, 557–566.
40. El-Amraoui, A., Schonn, J.-S., Küssel-Andermann, P., Blanchard, S., Desnos, C., Henry, J.-P., Wolfrum, U., Darchen, F. and Petit, C. (2002) MyRIP, a novel Rab effector, enables myosin VIIa recruitment to retinal melanosomes. *EMBO Rep.*, **3**, 463–470.
41. Gietz, R.D. and Woods, R.A. (2002) Screening for protein–protein interactions in the yeast two-hybrid system. *Methods Mol. Biol.*, **185**, 471–486.
42. Küssel-Andermann, P., El-Amraoui, A., Safieddine, S., Nouaille, S., Perfettini, I., Lecuit, M., Cossart, P., Wolfrum, U. and Petit, C. (2000) Vezatin, a novel transmembrane protein, bridges myosin VIIA to the cadherin–catenins complex. *EMBO J.*, **19**, 6020–6029.
43. El-Amraoui, A., Sahly, I., Picaud, S., Sahel, J., Abitbol, M. and Petit, C. (1996) Human Usher IB/mouse *shaker-1*; the retinal phenotype discrepancy explained by the presence/absence of myosin VIIA in the photoreceptor cells. *Hum. Mol. Genet.*, **5**, 1171–1178.
44. Sahly, I., El-Amraoui, A., Abitbol, M., Petit, C. and Dufier, J.-L. (1997) Expression of myosin VIIA during mouse embryogenesis. *Anat. Embryol.*, **196**, 159–170.